清華大學

Data-Driven Constraints on Chiral Magnetic Transport in Heavy-Ion Collisions

Au-Au 19.6 GeV and Pb-Pb 5.02 TeV

Yu Guo

with *A. Akridge*, *J. Liao*, *S. Shi*, *H. Xing* and *H. Zhang*

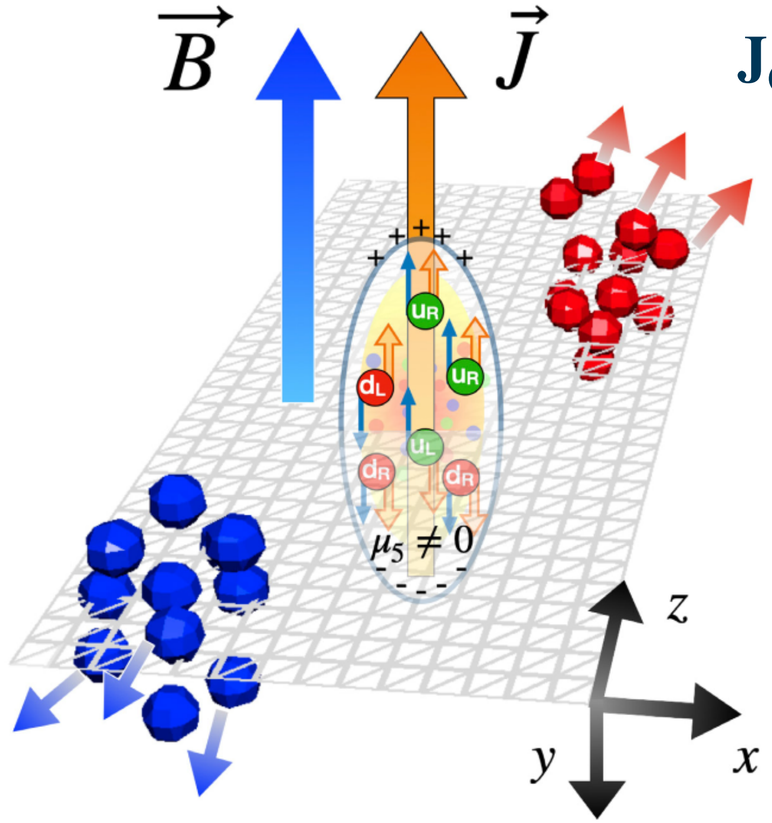
Department of Physics, Tsinghua University

Chirality 2026 · Zhuhai, China

Charge-dependent correlations and the CME background

CME-induced charge separation

Axial imbalance and magnetic field generate an electric current.

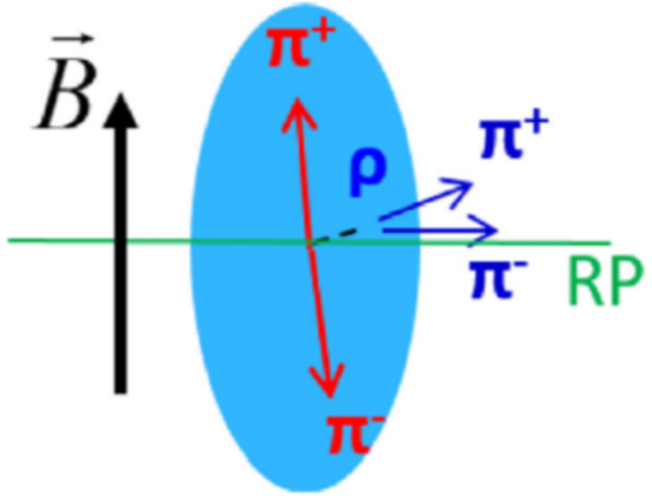


$$\mathbf{J}_{\mathrm{CME}} = C_A \mu_5 \mathbf{B}$$

[STAR Collaboration, Chinese Phys. C **50**, 094006 (2026)]

Charge-dependent background

Local charge correlations coupled to elliptic flow.



[J. Zhao et al, PPNP 107, 200 (2019)]

Charge-dependent particle correlations

$$\delta = \left\langle \cos(\phi_\alpha - \phi_\beta) \right\rangle, \qquad \gamma_{112} = \left\langle \cos(\phi_\alpha + \phi_\beta - 2\Psi_2) \right\rangle$$

$$\Delta\delta = \delta_{\mathrm{OS}} - \delta_{\mathrm{SS}}, \qquad \Delta\gamma = \gamma_{112,\mathrm{OS}} - \gamma_{112,\mathrm{SS}}$$

AVFD parameters and inference framework

AVFD parameters

$$\boldsymbol{\theta} = \left(\tau_B,\, f_{\mathrm{LCC}},\, n_5/s\right)$$

τ_B : Magnetic-field lifetime

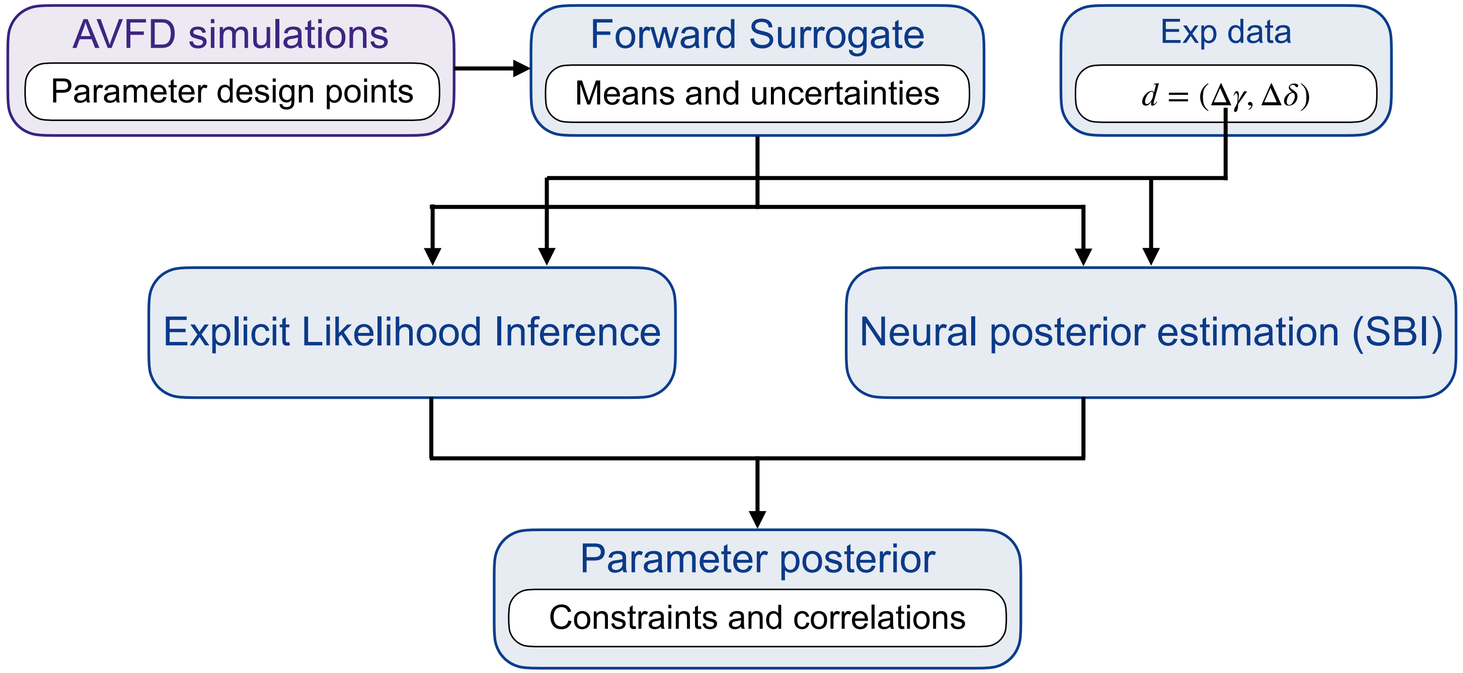
$$B(\tau, \mathbf{x}) = B_0(\mathbf{x}) \frac{\tau_B^2}{\tau^2 + \tau_B^2}$$

n_5/s : Initial axial charge strength density / entropy density

f_{LCC} : Local charge conservation

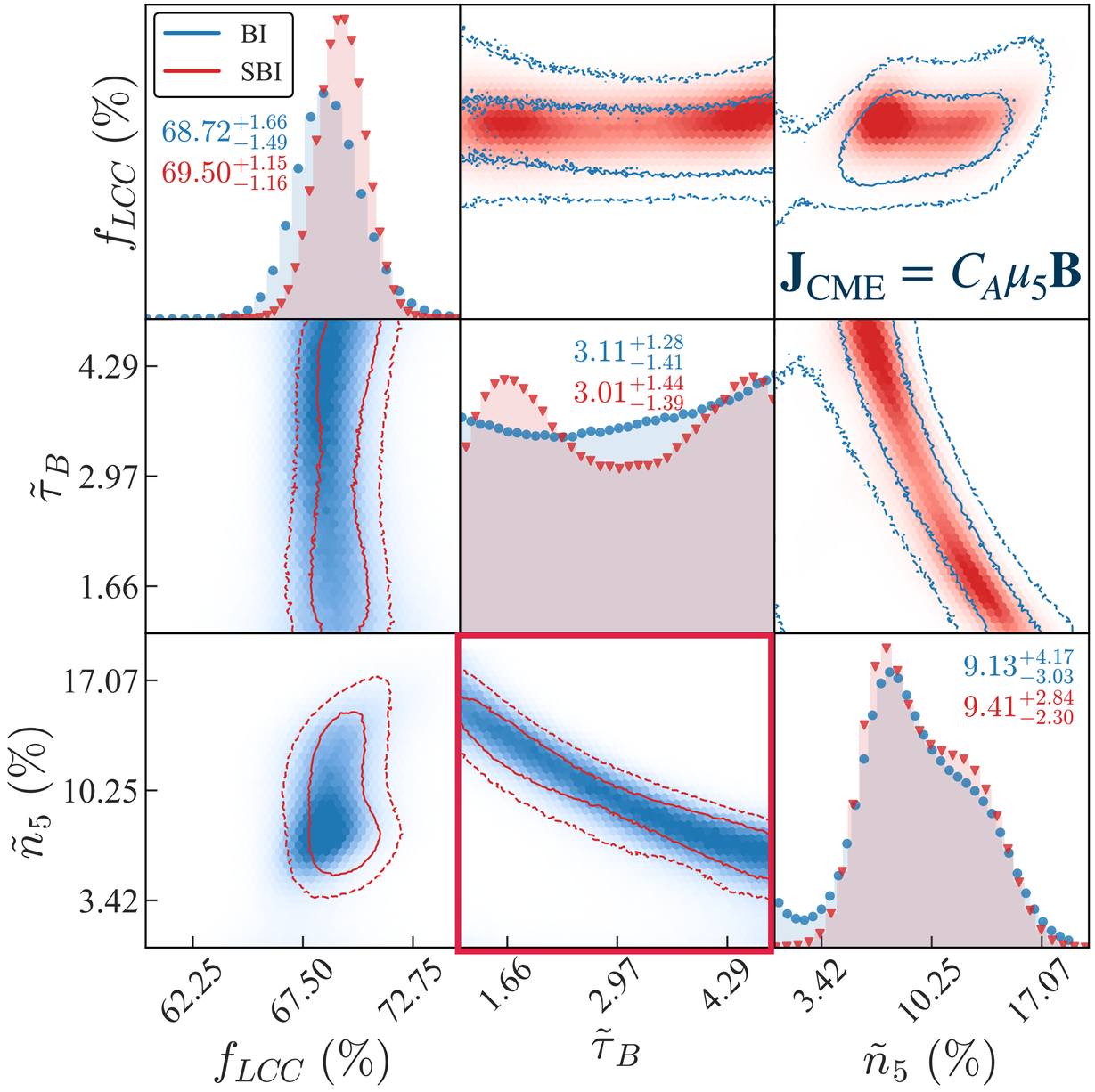
Controls local charge-balancing pair sampling.

Inference framework



$$\underbrace{p(\boldsymbol{\theta} \mid \mathbf{d})}_{\text{Posterior}} \propto \underbrace{p(\mathbf{d} \mid \boldsymbol{\theta})}_{\text{Likelihood}} \underbrace{\pi(\boldsymbol{\theta})}_{\text{Prior}}, \qquad \mathbf{d} = (\Delta\gamma, \Delta\delta)$$

AuAu 19.6 GeV parameter constraints



$$\tilde{\tau}_B = \frac{\tau_B}{2R/\gamma_{\mathrm{beam}}}, \qquad \tilde{n}_5 = \frac{n_5}{s}$$

LCC constraint

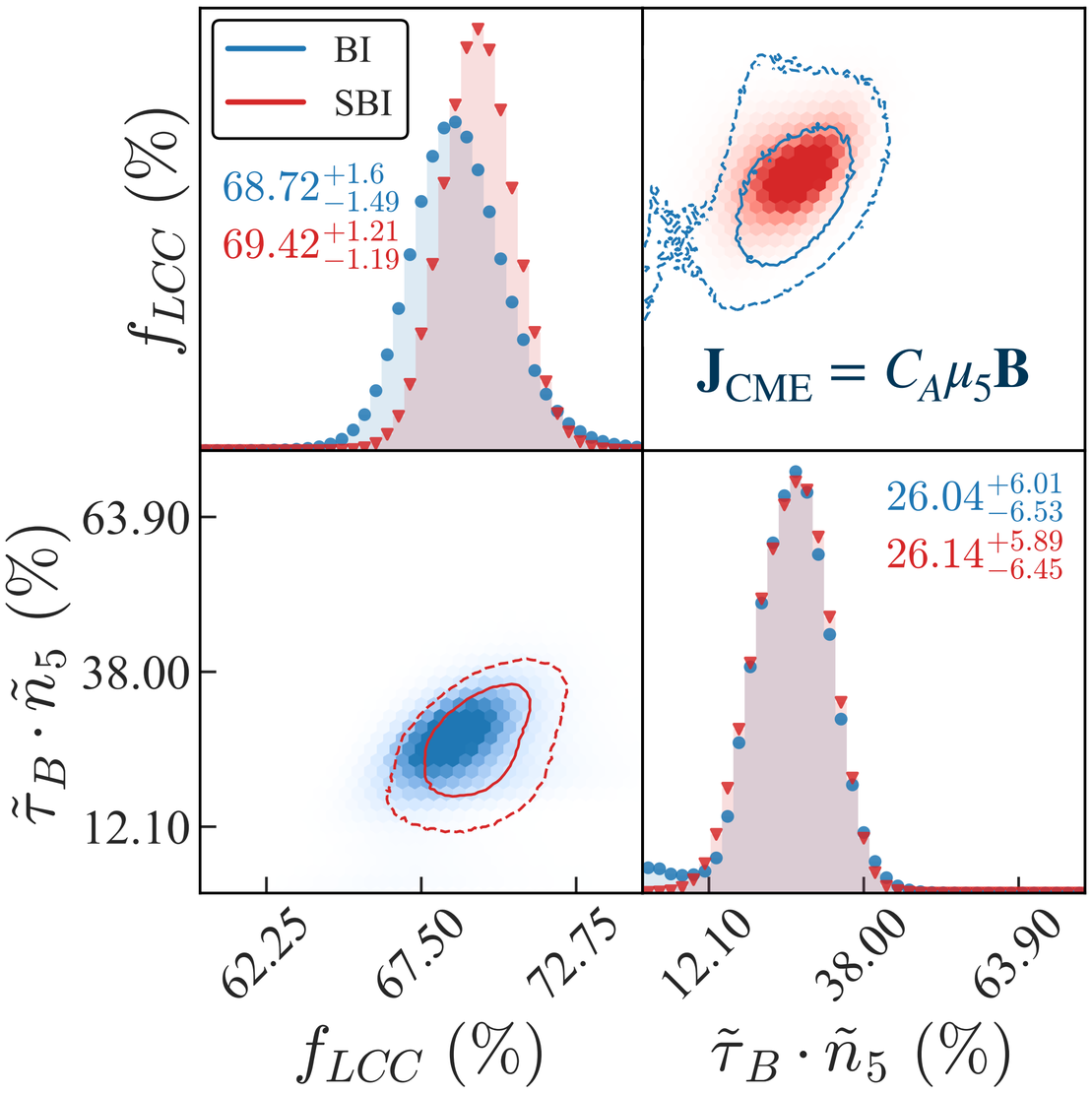
Both methods constrain f_{LCC} around 69%.

Parameter degeneracy

A longer magnetic-field lifetime can compensate for a smaller initial axial charge.

[STAR Collaboration, Phys. Rev. C **113**, 014912 (2026)]

Constraints on the combined parameter



$$\widetilde{P} = \tilde{\tau}_B \tilde{n}_5, \qquad \tilde{n}_5 = \frac{n_5}{s}$$

Calculated sample by sample from the joint posterior.

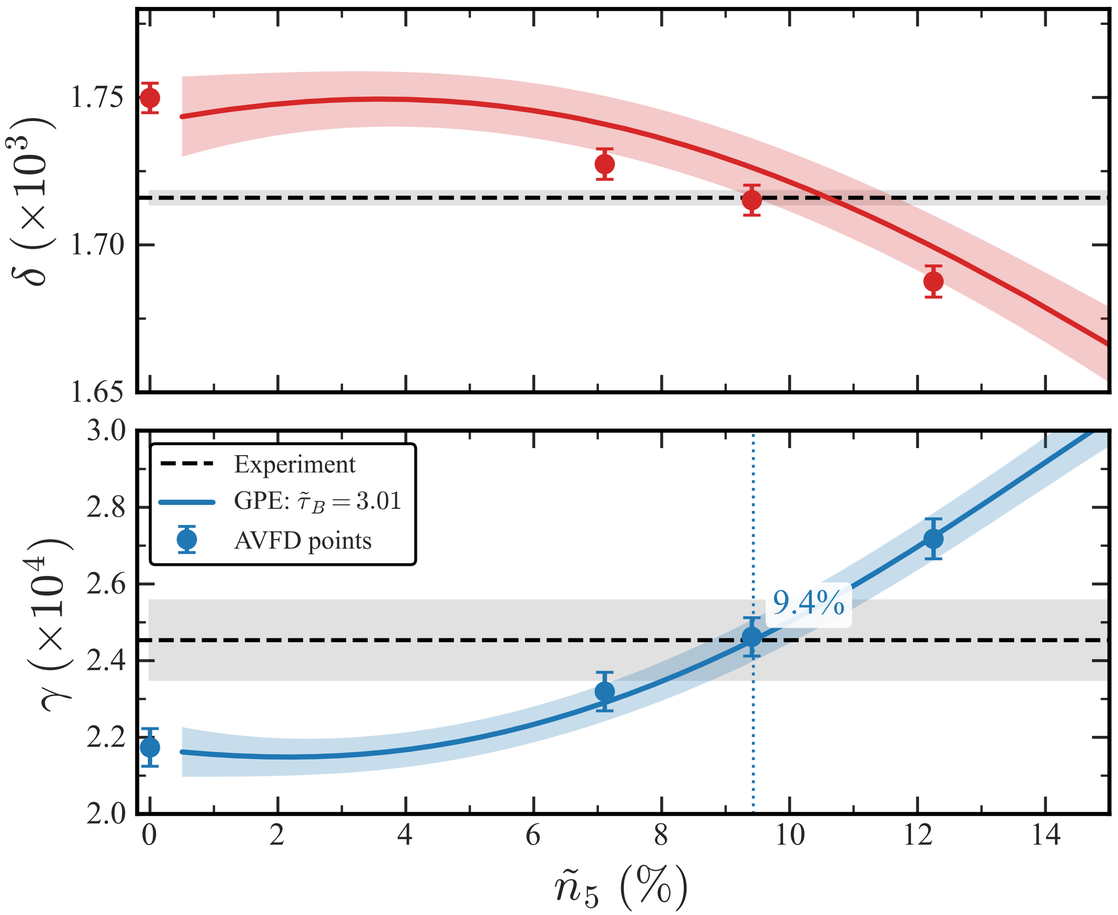
Single-peaked combined posterior
The product provides a useful summary of the parameter degeneracy.

Similar constraints from both methods

The combined parameter is not a direct estimate of the CME fraction.

Full AVFD checks of the inferred response

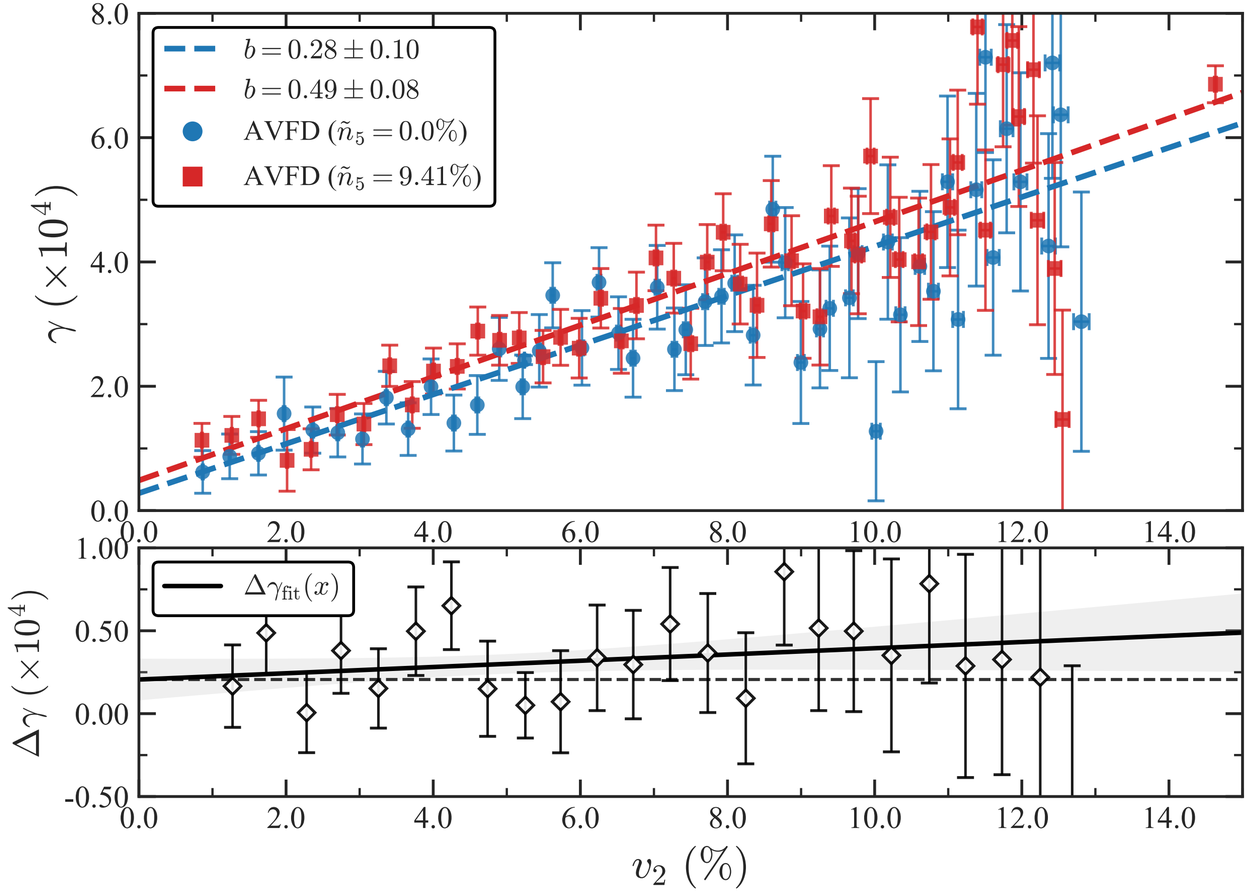
Integrated correlators



Fixed f_{LCC} and $\widetilde{\tau}_B = 3.01$.

$\widetilde{n}_5$: posterior median and 68% interval endpoints.

ESS estrapolation

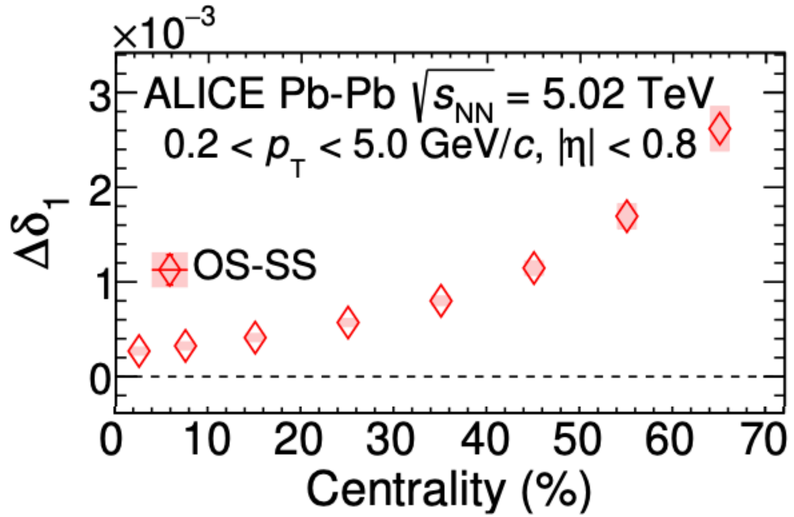


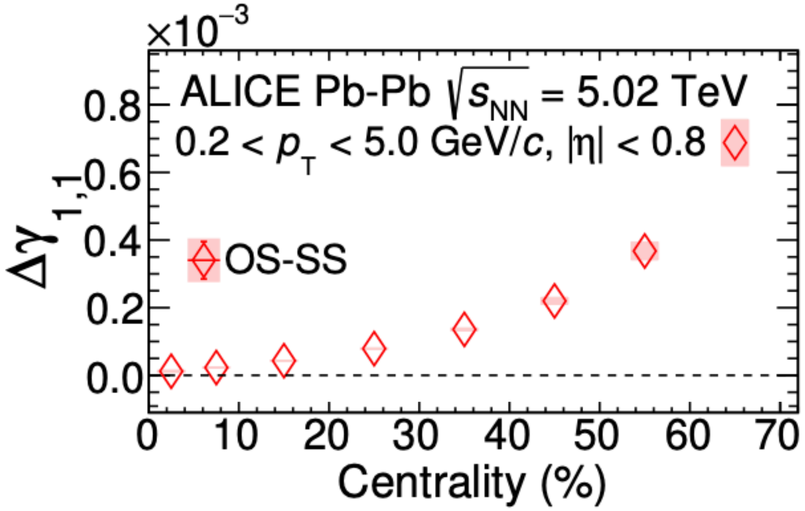
$$\Delta\gamma_{112}(v_2) = av_2 + b$$

$$b_{STAR} = (0.49 \pm 0.20) \times 10^{-4}$$

[STAR Collaboration, Phys. Rev. C **113**, 014912 (2026)]

Pb–Pb at 5.02 TeV: analysis setup





[ALICE Collaboration, JHEP 09 (2020) 160]

Calibration observables : $d = (\Delta\gamma_{112},\ \Delta\delta)$

Centrality selection

10-20%, 20-30%, 30-40%, 40-50%, 50-60%, 60-70%

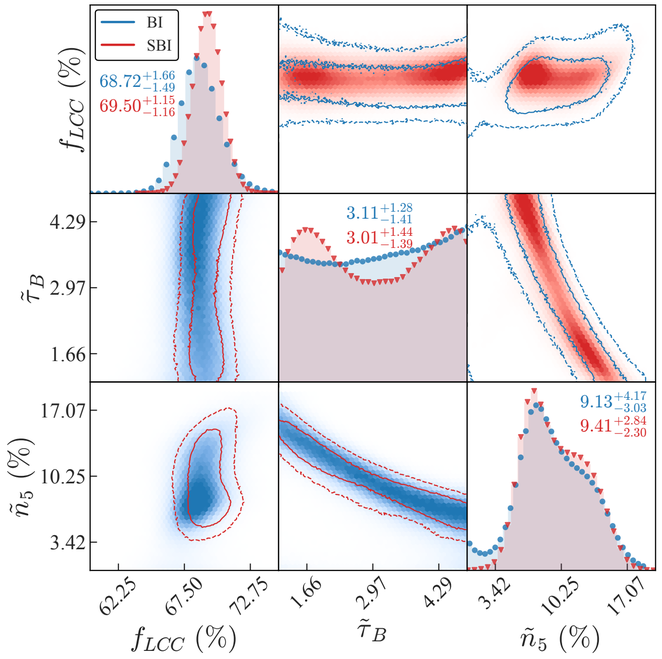
Further tests : differential observables at 30–40%.

Prior range

$0 \leq \tau_B \leq 0.3$ fm/c

$0 \leq f_{LCC} \leq 1$

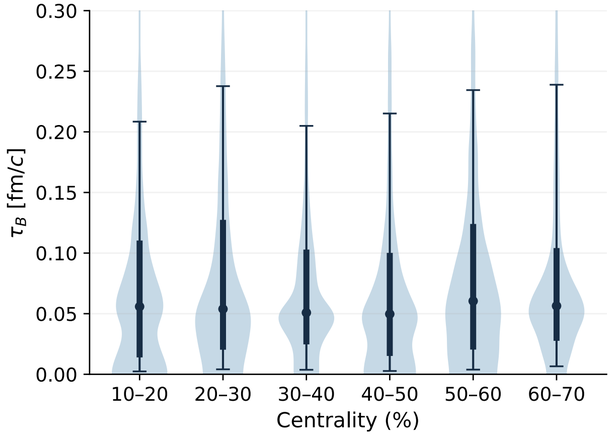
$0 \leq n_5/s \leq 0.5$

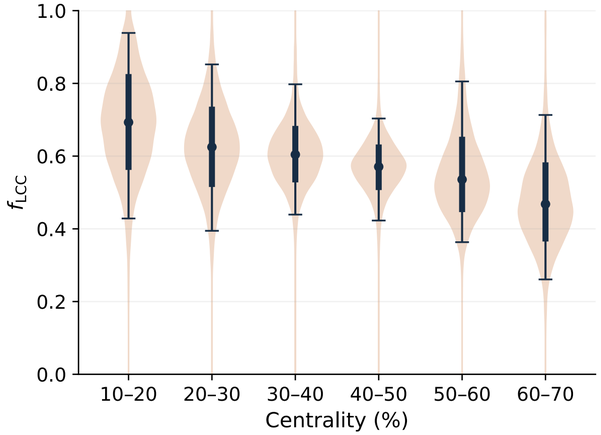


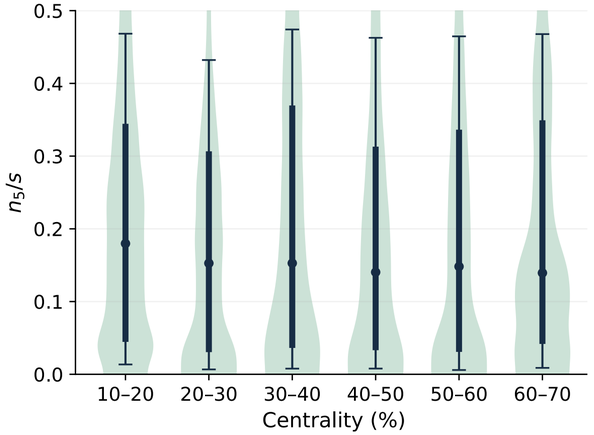
Centrality dependence of the inferred parameters

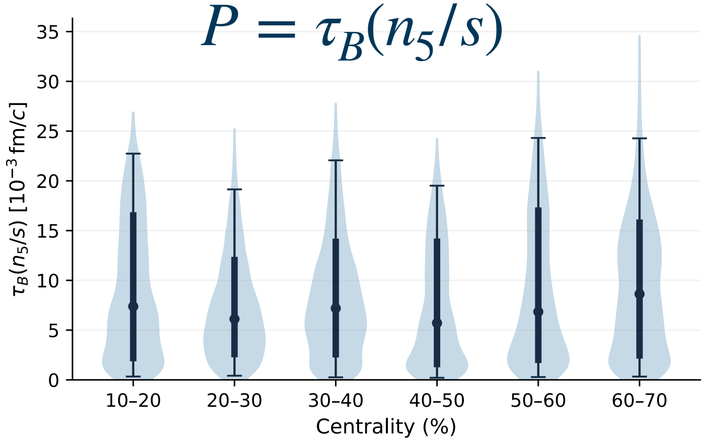
Preliminary

Points: Median and 68.27%/95.45% equal-tailed credible intervals.





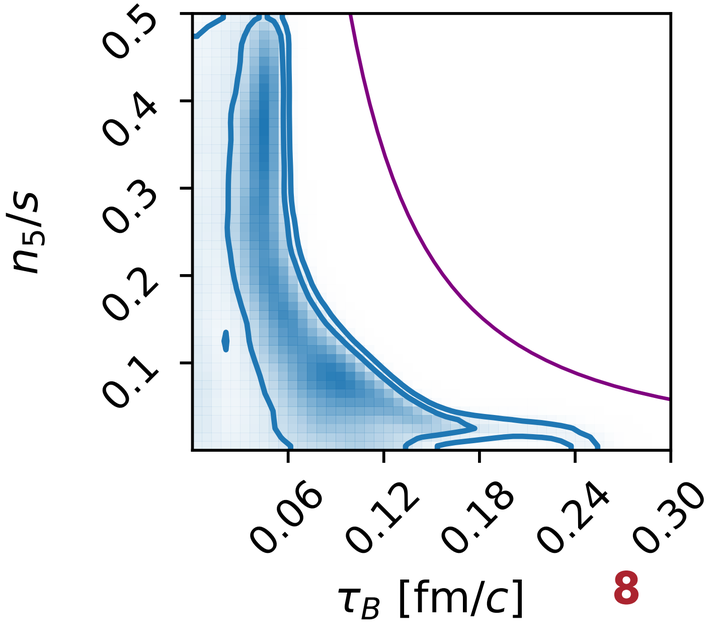




LCC trend: The median f_{LCC} decreases from approximately 0.69 to 0.47 toward peripheral collisions.

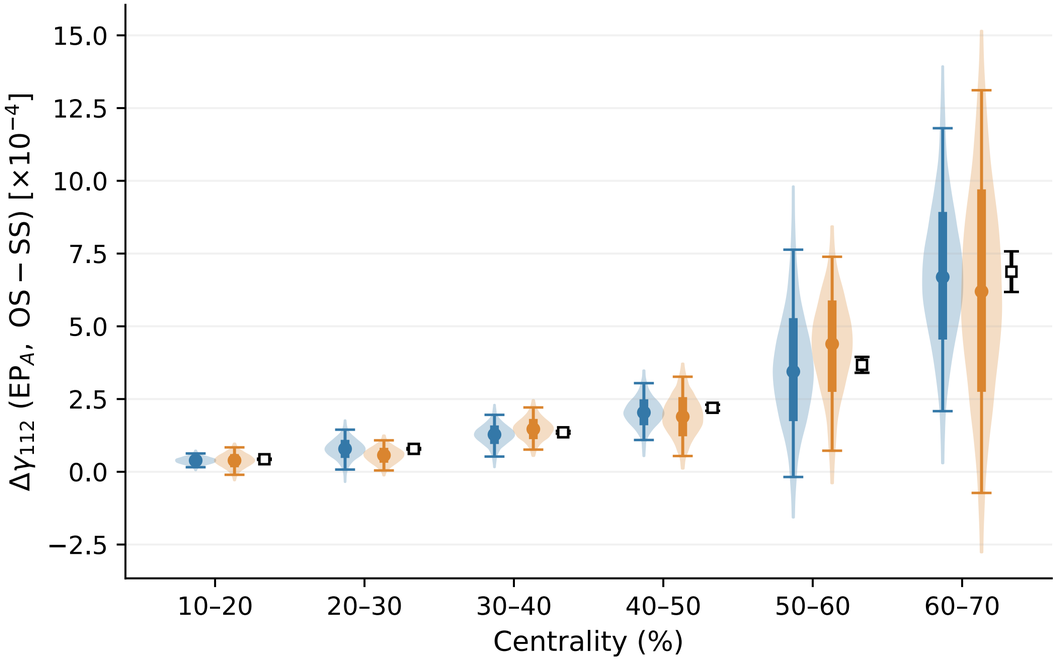
Parameter degeneracy: Broad marginal posteriors and a strong τ_B-n_5/s anticorrelation.

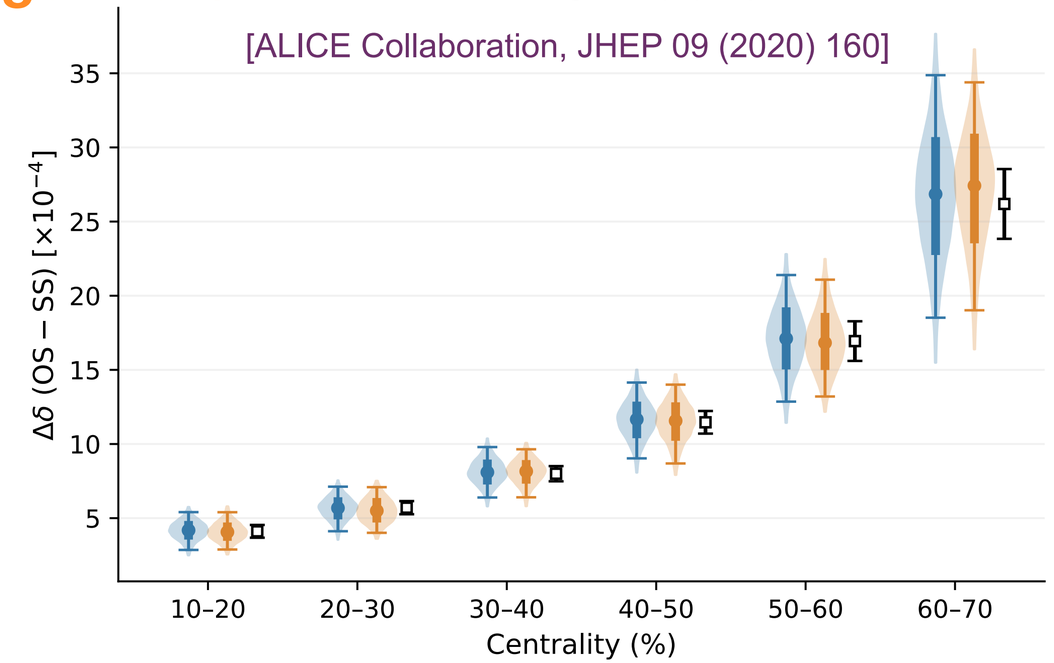
Combined parameter: No clear monotonic centrality trend in $P = \tau_B(n_5/s)$.



CME-allowed and no-CME predictions

Blue: CME allowed **Orange: No CME** **□ ALICE data** *Preliminary*





Models

M_1: CME allowed, $\theta = (\tau_B, f_{LCC}, n_5/s)$.

M_0: No CME, $\tau_B = n_5/s = 0, f_{LCC}$ fitted.

Posterior predictive check

Model uncertainty and experimental noise included

Same data used for calibration and comparison

Both models describe the fitted data within current uncertainties.

Model comparison provides no clear preference

Preliminary

Bayes factors

Centrality	B_10	ln B_10
10-20%	0.839	-0.175
20-30%	0.796	-0.228
30-40%	0.423	-0.861
40-50%	0.676	-0.392
50-60%	0.490	-0.714
60-70%	1.080	0.077

Bayesian evidence

$$Z_M = \int \mathscr{L}(\mathbf{d} \mid \theta, M)\, \pi(\theta \mid M)\, d\theta, \qquad B_{10} = \frac{Z_1}{Z_0}.$$

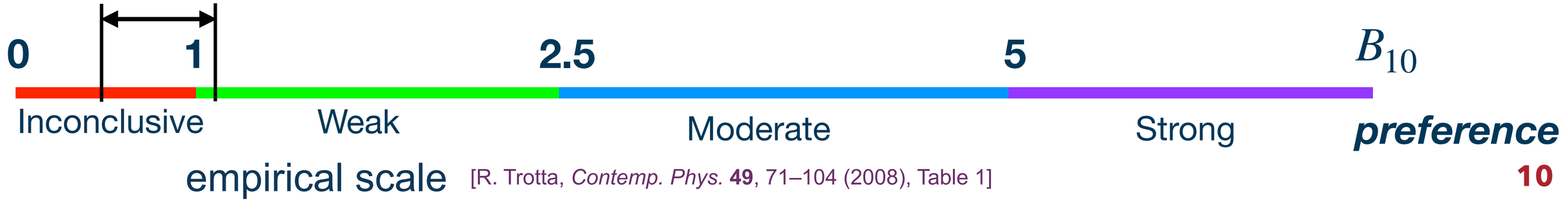
M_1: CME allowed,

M_0: No CME.

$B_{10} > 1$: favors M_1

$B_{10} < 1$: favors M_0

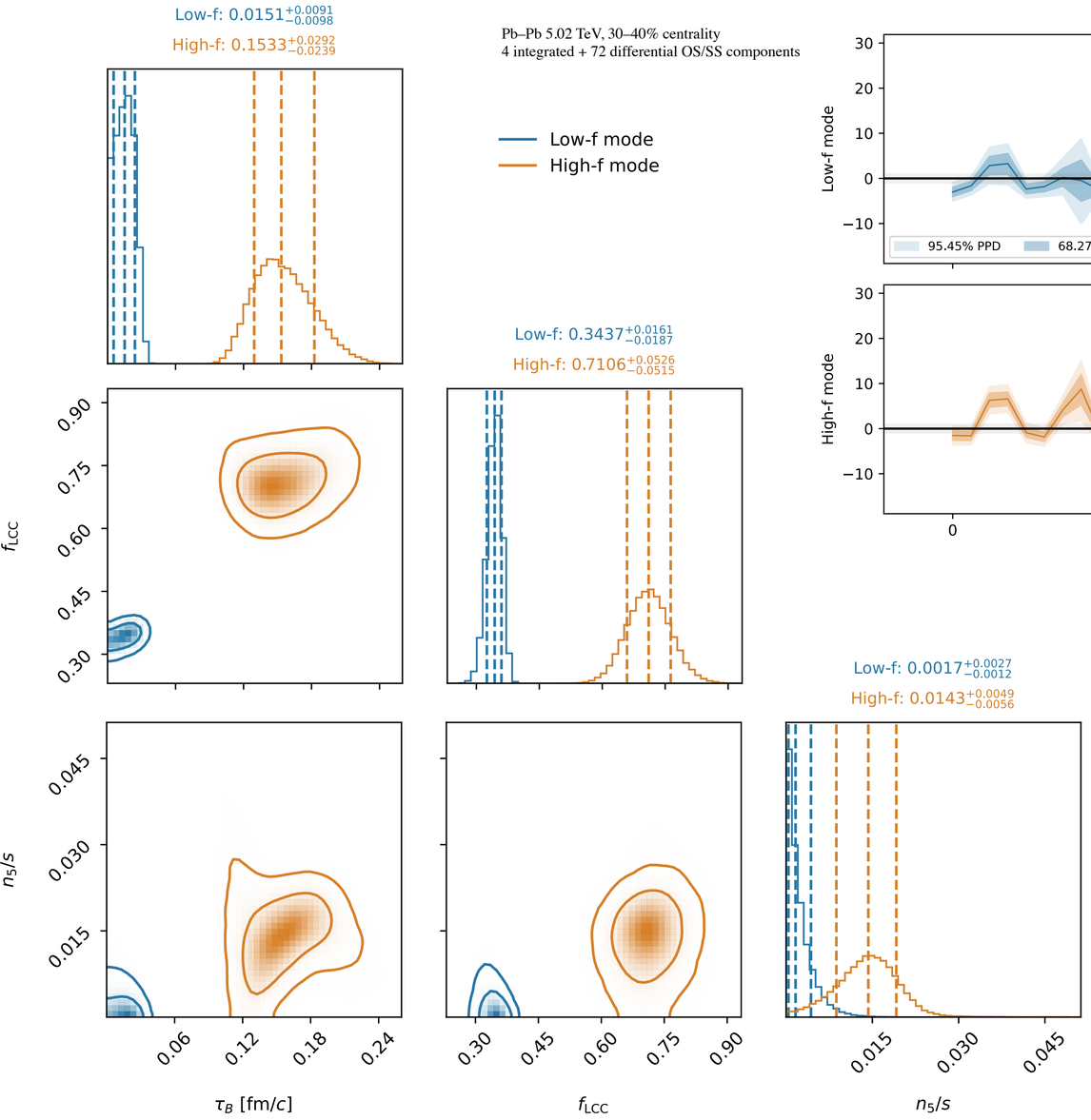
$0.42 \leq B_{10} \leq 1.08$



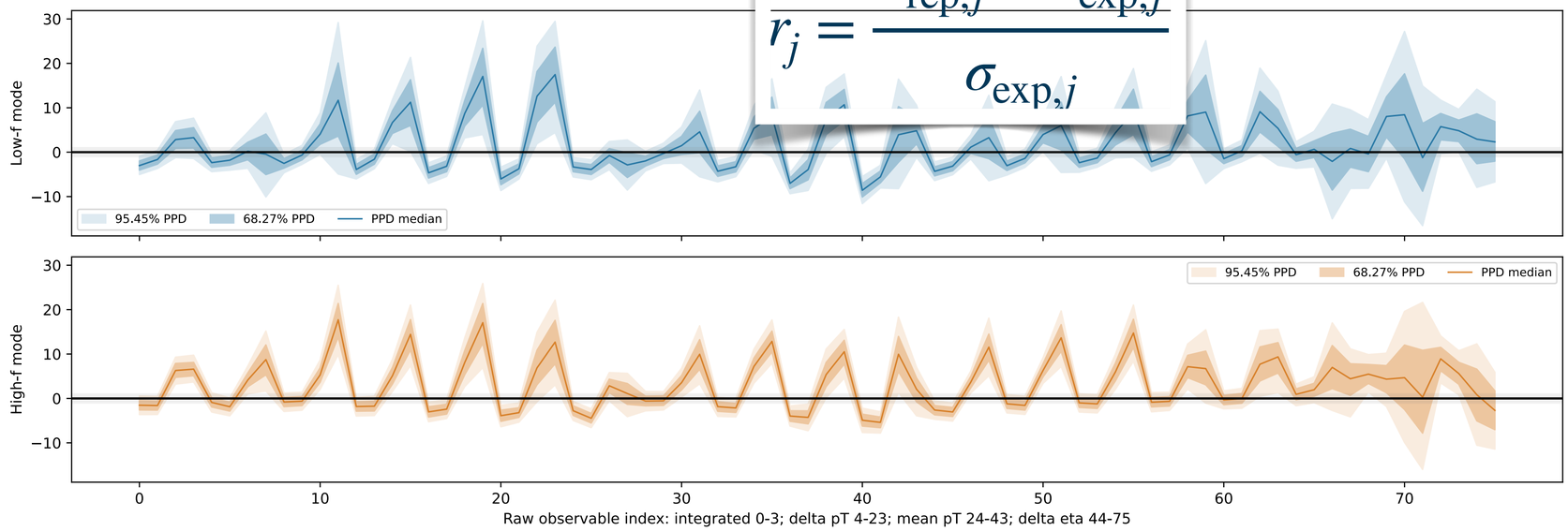
empirical scale [R. Trotta, *Contemp. Phys.* **49**, 71–104 (2008), Table 1]

Differential observables: unresolved discrepancies

Preliminary



$$r_j = \frac{d_{\mathrm{rep},j} - d_{\mathrm{exp},j}}{\sigma_{\mathrm{exp},j}}$$



Two separated candidate branches

Distinct low- and high-f_{LCC} solutions

Neither branch describes all 76 components simultaneously

Further checks of event statistics, GPE coverage, and observable covariance are needed.

Summary

BES: parameter degeneracy

- BI and SBI yield similar constraints on $\widetilde{\tau}_B(n_5/s)$.
- Selected-point AVFD calculations give an ESS intercept compatible with STAR.

LHC: no clear model preference — Preliminary

- The median f_{LCC} decreases toward peripheral collisions.
- Neither model is clearly preferred: $0.42 \leq B_{10} \leq 1.08$, conditional on current priors and uncertainties.

Differential fit: further validation needed

- Break degeneracy.
- But neither candidate branch describes all 76 components simultaneously.